Nano Research 2018, 11(5): 2405–2411
https://doi.org/10.1007/s12274-017-1861-3
Research Article
ISSN 1998-0124
CN 11-5974/O4

Single Cr atom catalytic growth of graphene

Huy Q. Ta[1,2,3,§], Liang Zhao[1,2,§], Wanjian Yin[1,2] (✉), Darius Pohl[4], Bernd Rellinghaus[4], Thomas Gemming[4], Barbara Trzebicka[3], Justinas Palisaitis[5], Gao Jing[1,2], Per O. Å. Persson[5], Zhongfan Liu[1,2,6], Alicja Bachmatiuk[1,2,3,4] (✉), and Mark H. Rümmeli[1,2,3,4] (✉)

[1] *Soochow Institute for Energy and Materials Innovations, College of Physics, Optoelectronics and Energy & Collaborative Innovation Center of Suzhou Nano Science and Technology, Soochow University, Suzhou 215006, China*
[2] *Key Laboratory of Advanced Carbon Materials and Wearable Energy Technologies of Jiangsu Province, Soochow University, Suzhou 215006, China*
[3] *Centre of Polymer and Carbon Materials, Polish Academy of Sciences, M. Curie-Sklodowskiej 34, Zabrze 41-819, Poland*
[4] *IFW Dresden, Helmholtz Strasse 20, 01069, Dresden, Germany*
[5] *Department of Physics, Chemistry and Biology (IFM), Linköping University, SE-581 83 Linköping, Sweden*
[6] *Center for Nanochemistry, Beijing Science and Engineering Centre for Nanocarbons, Beijing National Laboratory for Molecular Sciences, College of Chemistry and Molecular Engineering, Peking University, Beijing 100871, China*
[§] *Huy Q. Ta and Liang Zhao contributed equally to this work.*

Received: 1 August 2017
Revised: 12 September 2017
Accepted: 20 September 2017

KEYWORDS
in situ transmission electron microscope (TEM),
electron driven catalysis,
Cr,
single atom,
graphene synthesis

ABSTRACT

Single atoms are the ultimate minimum size limit for catalysts. Graphene, as an exciting, ultimately thin (one atom thick) material can be imaged in a transmission electron microscope with relatively few imaging artefacts. Here, we directly observe the behavior of single Cr atoms in graphene mono- and di-vacancies and, more importantly, at graphene edges. Similar studies at graphene edges with other elemental atoms, with the exception of Fe, show catalytic etching of graphene. Fe atoms have been shown to both etch and grow graphene. In contrast, Cr atoms are only observed to induce graphene growth. Complementary theoretical calculations illuminate the differences between Fe and Cr, and confirm single Cr atoms as superior catalysts for sp^2 carbon growth.

1 Introduction

The current revolution in the synthesis of two-dimensional (2D) materials dictates a core need for their synthesis with atomic precision, as by their very nature, 2D materials' structure–property relationships are sensitive at the single atomic level [1]. Thus, synthesis/engineering approaches for such materials

Address correspondence to Mark H. Rümmeli, mhr1@suda.edu.cn; Alicja Bachmatiuk, alicja-bachmatiuk@wp.pl; Wanjian Yin, wjyin@suda.edu.cn

need to eventually provide atomic precision. Post-engineering approaches can be considered top down, while straightforward synthetic approaches are bottom up [1, 2]. Moreover, the most successful synthetic approaches all use catalysts. The ultimate catalyst is a single atom, as it maximizes catalytic efficiency [3–5]. In addition, it potentially offers growth precision at the atomic scale. In order to achieve such control, it is of key importance to understand how single atoms (usually transition metals) interact with unsaturated bonds from the 2D material, in particular, the addition and removal of the 2D material being grown. To date, most studies have been conducted with graphene, as this is the godfather of 2D materials. Numerous studies have examined atoms in graphene vacancies, in particular, using aberration-corrected transmission electron microscopy (TEM), which allows one to examine single-atom layers without significant imaging artefacts. Examples can be found in a review article by Sun et al. [6]. Studies examining single atoms at the edges of graphene are fewer. Most of these demonstrate the catalytic etching of graphene. Examples for the catalytic etching of graphene by single atoms under electron beam irradiation include Cr, Ti, Pd, Ni, Al, and Au with a condensed scanning electron beam [7], and Si with a parallel imaging beam [8]. Fe atoms, on the other hand, have been observed to both etch and grow graphene under a parallel electron beam in TEM [3]. In this work we examine Cr atoms in graphene vacancies and at graphene edges while under electron beam irradiation in a TEM with an electron acceleration voltage of 80 kV. We compare the behavior of the Cr atoms in vacancies and at graphene edges with the published data for Fe [3, 9] and with complementary theoretical calculations. Cr is shown to be a more stable and efficient catalytic atom than Fe.

2 Result and discussion

Initially, we examine single Cr atoms incorporated in single and double vacancies in graphene, then focus on the catalytic growth of graphene by Cr atom(s) at graphene open edges. Details of the sample preparation are provided in the supplementary information, as well as in a previous report [10]. In brief, graphene grown over Cu by chemical vapor deposition (CVD) was transferred to a lacy carbon-Cu TEM grid. The grid and graphene were then placed in a vial with a nominal amount of Cr acetylacetonate (acac). The vial was evacuated to ~ 10^{-6} mbar and then sealed. The sealed vial was then annealed at 170 °C for 12 h, during which the $Cr(acac)_3$ sublimes and decomposes, leaving Cr on the graphene surface. Energy-dispersive X-ray (EDX) spectroscopy and local electron energy loss spectroscopy (EELS) were carried out to confirm the deposited material on the graphene is chromium [10] (Fig. S1 in the Electronic Supplementary Material (ESM)). Moreover, to further confirm the atoms we observe in this TEM study are Cr rather than Cu (from the CVD-grown graphene over Cu), Fe (from the FeCl etchant to remove Cu during the transfer process), or Si from the CVD reaction tube, we compared the relative intensities of the C-Cr atoms in the TEM micrographs with those from the multislice image simulations for Cr, Cu, Fe, and Si (see Fig. S2 in the ESM) [9, 10]. The relative intensities comparison is also in agreement with the analytical studies confirming that the observed atoms in our study are Cr.

Figure 1 shows the two types of vacancy states that we commonly observed of Cr atoms embedded in graphene, namely, single vacancies (Fig. 1(a)) and divacancies (Fig. 1(d)). Supporting image simulations (Figs. 1(b) and 1(e)) confirm the structure of the defect

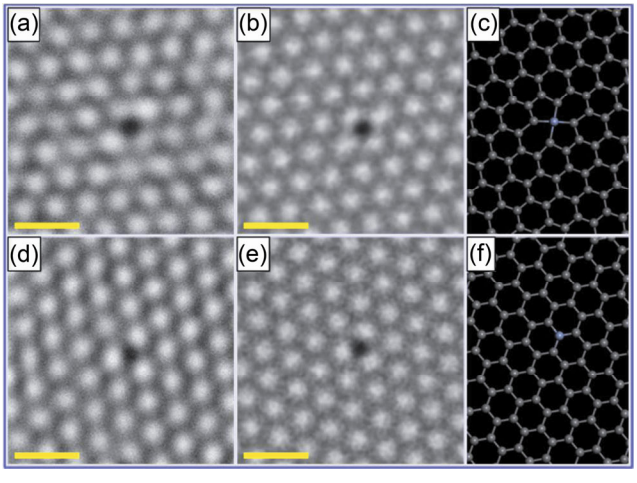

Figure 1 Configuration of a single Cr atom in graphene single- and double-vacancies. (a)–(c): HRTEM image, image simulation, and stick-and-ball model of a single Cr atom at a graphene double vacancy (DV). (d)–(f): HRTEM image, image simulation, and stick-and-ball model of a single Cr atom at a graphene single vacancy (SV). Scale bar = 5 Å.

(Figs. 1(c) and 1(f)) for single and divacancies, respectively. Various other examples can be found in Figs. S3 and S4 in the ESM.

These defects are similar to those found for Fe atoms in graphene by the Warner group [9]. In that study, they also used parallel electron illumination at 80 kV, and the Fe atoms were shown to migrate relatively easily. In our case, though the current density of our electron beam is several orders of magnitude larger (nA as opposed to pA), for the most part the defects were stable even after irradiation for well over 60 s (Fig. S5 in the ESM). Only once did we observe a Cr atom migrate from a vacancy. This is presented in Fig. 2, and shows that the Cr atom exchanges position with a carbon atom (Figs. 2(a) and 2(b)). Supporting image simulations and stick-and-ball models confirm the Cr configuration in a single vacancy in the graphene (Figs. 2(c), 2(e) and 2(f) respectively). This is rather different from the case for Fe atoms, where it was shown that the divacancies can reconstruct relatively easily to change their orientation, or even change to a single vacancy configuration (Fig. 2(g)). Given the stability of the Cr atoms in our irradiation studies with higher electron current densities compared to Fe atoms, this suggests a larger binding energy for Cr than for Fe.

First-principle calculations based on the density functional theory (DFT) were implemented to investigate both the energetic and kinetic stability of Cr and Fe in both mono- and divacancy configurations. For energetic stability, the binding energy (E_b) is defined as

$$E_b = (E(A) + E(Gr\text{-}V)) - E(A+Gr\text{-}V) \quad (1)$$

where E(A), E(Gr-V), and E(A+Gr-V) are the total energies of single Cr or Fe atoms, graphene with a mono- or divacancy, and a Cr or Fe atom embedded in the graphene vacancy, respectively. The DFT calculations showed a slightly higher binding energy for Cr as compared to Fe. For single vacancies, the binding for Cr and Fe are 10.165 and 10.005 eV, respectively, while for di-vacancies they are 8.663 and 8.210 eV. With regard to kinetic stability, we used the nudged elastic band (NEB) approach to compare the energy barrier for the site exchange (Cr-C) for a single vacancy. The data (Fig. 2(h)) shows the process is more

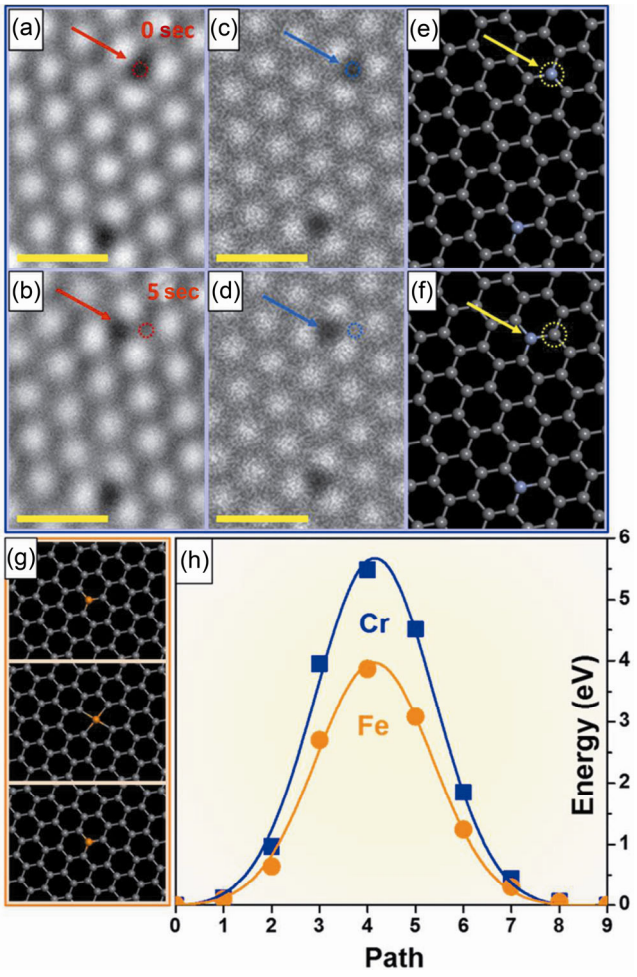

Figure 2 Site exchange between single Cr and C atoms, single vacancy, while under electron beam irradiation. (a) and (b): HRTEM images of single Cr atom at graphene SV before and after exchange. Image simulations (c), (d), and stick-and-ball models (e), (f) correspond to the TEM images in panels (a) and (b), respectively. Arrows indicate the position of the Cr atom before and after exchange, dotted circles indicate the original position of the Cr atom. (g): Stick-and-ball models showing the exchange of an Fe atom between a single vacancy and a double vacancy. This behavior was not observed with Cr. (h): Energy barrier comparison for SV site exchange between Cr (blue) and Fe (orange) atom. Scale bar = 5 Å.

difficult (larger barrier) for Cr than for Fe, which is consistent with the calculated larger binding energy for Cr than for Fe. Both the energetic and kinetic stability calculations suggest that Cr atoms in graphene vacancies are more stable than Fe atoms.

We now turn to the dynamic behavior of single Cr atoms at the edge of graphene. Typically, the atoms at graphene edges migrate in no particular direction along the graphene edge while irradiated. The captured migrations (1 frame per second) upon closer examination,

for all our observations across nine different studies, show that after migration, new carbon atoms had been inserted between the Cr atoms' initial and final positions, forming new hexagonal structures at the graphene edge, leaving a zig-zag edge termination.

A zig-zag edge termination is not unexpected, as this is the lowest energy configuration compared with armchair or chiral edge terminations [11]. An example of this process with additional micrographs to highlight the incorporated C atoms upon Cr migration can be seen in Fig. 3. Further examples are provided in Figs. S6 and S7 in the ESM. A simple statistical analysis of the number of new hexagons forming at the open graphene edge varied between one and six for a one-frame-per-second micrograph capture rate. At times, several Cr atoms in close vicinity could be observed to migrate, and in a similar fashion to single Cr atoms, new carbon hexagons were observed at the graphene edge (see, for example, Fig. S8 in the ESM).

The fact that we always encountered graphene growth under the conditions in which we observe the Cr atoms is remarkable. This is not only because the catalytic role of a single atom is usually to etch graphene, but also because under these conditions, the electron beam can sputter the unsaturated graphene edge atoms [12]. The *in situ* electron microscopy data suggests that Cr atoms are highly efficient as single-atom catalysts for the growth of graphene.

To better comprehend the catalytic role of Cr atoms on graphene, we conducted molecular dynamic (MD) simulations for both Fe and Cr, as Fe atoms have been shown to also catalytically grow graphene, albeit less efficiently [3]. Figure 4 summarizes the MD data. The MD simulations show catalytic growth for both Cr (Figs. 4(a)–4(d)) and Fe (Figs. 4(e)–4(h)), where new hexagon structures form at the graphene edge as new C is added. A more in-depth analysis of the Cr and Fe atoms diffusion at the graphene edge shows that Fe is significantly more dynamic than Cr, both from a temporal and spatial perspective. Over the examined time frame, the maximum diffusion distance for Cr does not exceed 8 Å, whereas Fe reaches well over three times that (28 Å). In addition, the oscillatory frequency of Cr at a graphene edge is far less than that of Fe. This data is presented in Figs. 4(i) and 4(j) for Cr and Fe, respectively. The significant difference between Fe and Cr can be attributed to their energetic and kinetic stability, as discussed above.

An efficient single-atom catalyst should have a good balance between stability and migration. Stability is required as a nucleation site so as to attract additional C atoms for the catalytic growth process, while the ability to migrate is necessary to keep the catalyst atom active along the graphene edge and avoid poisoning. Our MD simulations show that Cr is relatively stable (with an average stability of ~ 4.0 ns before migration) but still capable of diffusing, while Fe is less stable

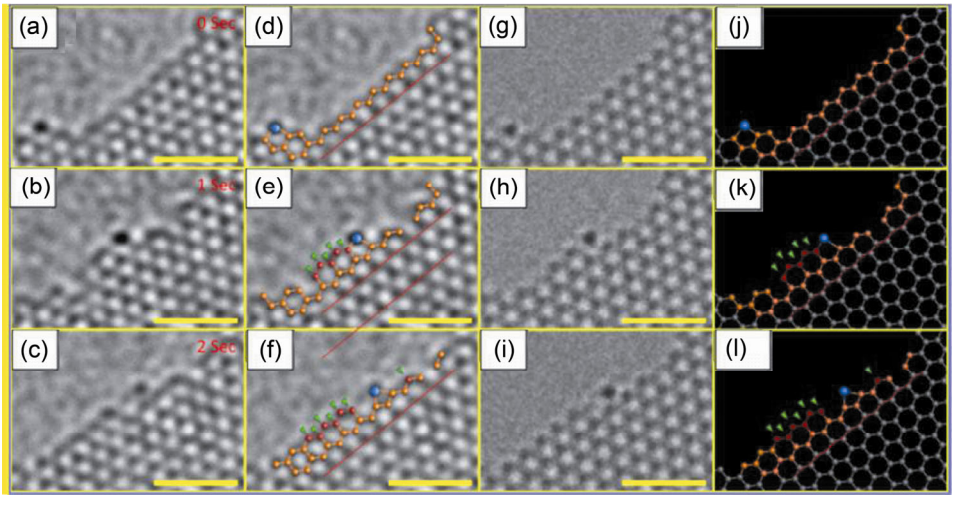

Figure 3 Catalytic growth of graphene by a single Cr atom at the graphene edge under electron beam irradiation. (a)–(c), with partial stick-and-ball models to aid viewing (d)–(f), image simulations of the growth process (g)–(i), and complete stick-and-ball models (j)–(l). The blue ball indicates Cr, whereas red balls and green arrows signify new C atoms. All scale bars are 1 nm.

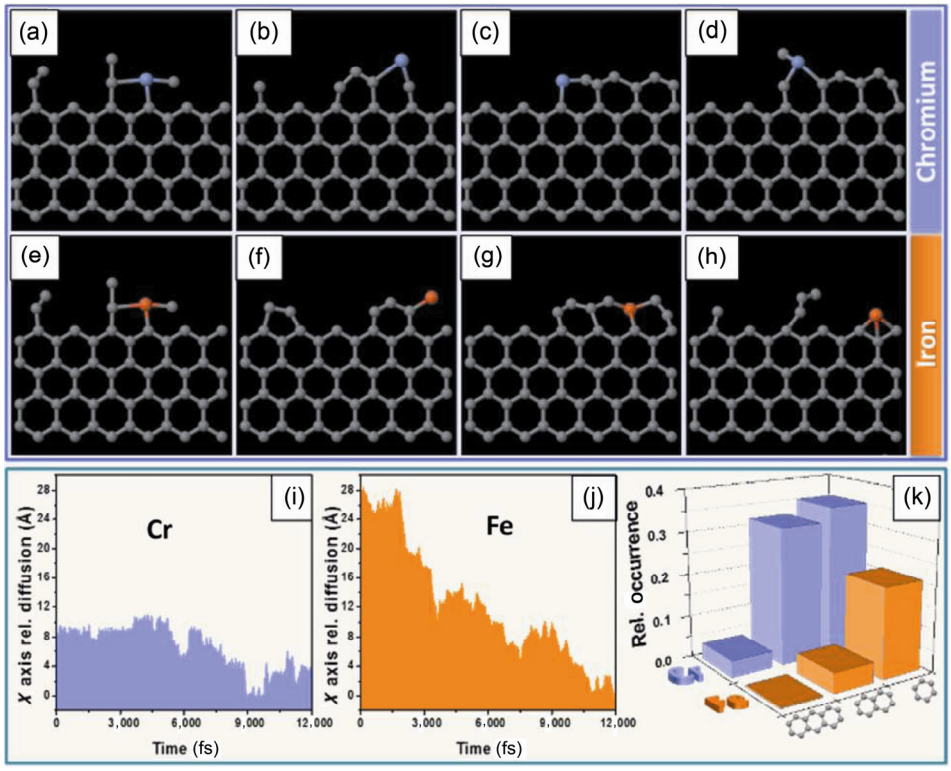

Figure 4 Stick-and-ball models from MD simulations for a Cr atom (a)–(d) and Fe atom (e)–(h) at a graphene edge, showing catalytic growth of graphene. Comparison of the diffusion activity of Cr and Fe atoms at the graphene edge (i), (j) and relative occurrence of new hexagon formation at the graphene edge (k).

(with an average stability of < 1 ns before migration) and hence less efficient as a nucleation catalyst. We also examined the occurrence of new hexagon formation at the graphene edge for the cases of Cr and Fe, presented in Fig. 4(k). The relative occurrence of new hexagon formation for single-, double-, and triple-hexagon formation was significantly more frequent for the case of Cr than Fe, indicating that Cr is a more efficient single-atom catalyst for graphene growth than Fe.

3 Conclusion

This finding is particularly interesting when one considers that pure Fe is an exceedingly good catalyst for carbon nanotube [13, 14] and multi-layer graphene [15] growth by CVD. There is almost nothing in the literature for Cr; we found only one article indicating carbon nanotube/fiber growth, and the authors highlighted that growth from Cr differed from the other transition metal catalysts [16].

While here we examine only a single Cr atom (against Fe), we postulate that Cr may also be highly capable as a catalyst to add C to a growing carbon nanotube/fiber as a cluster, but that the rate of carbon incorporation relative to carbon removal is so high that the catalyst cluster is overwhelmed by excess carbon addition, and is, in essence, poisoned. The concept of poisoning without carbon etching is well known, and it is for this reason that etchants are often added into the reaction for efficient carbon nanotube growth [17]. Hence, it may be that when using pure Cr clusters for carbon nanotube growth, sufficient etchants need to be included in the reaction. However, as a single atom under our *in situ* TEM conditions, Cr is a highly efficient catalyst for sp^2 carbon growth.

4 Methods

4.1 Sample preparation

Two graphene samples were prepared by thermal CVD over Cu foil [18]. The graphene was then

transferred onto standard Cu lacy carbon TEM grids. The transfer involved spin coating the graphene with PMMA and then etching the Cu foil away with $FeCl_3$. The PMMA graphene was then transferred to the TEM grid after the poly(methyl methacrylate) (PMMA) was removed with hot acetone vapor. The sample was then annealed in high vacuum (~ 10^{-6} mbar) overnight at 250 ˚C to minimize PMMA residue. After this, the TEM grid/graphene sample was placed in a quartz vial with a nominal amount of $Cr(acac)_3$ and evacuated to ~ 10^{-6} mbar. The quartz vial was then sealed and annealed at 175 ˚C This process sublimes and decomposes the $Cr(acac)_3$ to deposit Cr atoms on the graphene. X-ray dispersion spectroscopy and electron energy-loss spectroscopy confirmed the presence of Cr on the graphene.

4.2 TEM studies

An FEI Titan cubed with a Cs corrector for the objective lens was used. The electron acceleration voltage was 80 kV and the current density was typically 3.8 nA/nm^2. The multislice high-resolution TEM image simulations were conducted using JEMS software. All the simulation parameters were equivalent to those used in the TEM experiments. The acceleration voltage was 80 kV. The energy spread was set to 0.2 eV. A chromatic aberration, Cc, of 1 mm was set, and the spherical aberration, Cs, was set at 1 μm. Typically, the focus was 2–3 nm with a defocus spread of 2 nm. Low-pass filtering was applied to the micrographs to reduce noise. The filtering does not affect the final resolution of the images.

4.3 Image simulation

All image simulations used the same parameters and conditions to those used in the TEM experiments. The multislice HRTEM image simulations were implemented using JEMS software. An accelerating voltage of 80 kV (energy spread of 0.2 eV) was used for the simulations. Cc and Cs were fixed to 1 mm and 1 μm, respectively. A defocus of 2–3 nm and defocus spread of 2 nm was implemented. These values are consistent with the experimental conditions used.

4.4 Theoretical calculations

The first-principle calculations were carried out by using the VASP code [19, 20] with the standard frozen-core projector augmented-wave (PAW) method. The cut-off energy for the basis functions was 400 eV. The general gradient approximation of Perdew, Burke, and Ernzernhof (PBE) [21] was used for functional exchange-correlation. For energetic calculations, the atomic positions are fully relaxed for each calculation. The k-points mesh was chosen such that the product of the number of k-points and the corresponding lattice parameter is at least 40 Å. The MD simulations are performed based on the Born–Oppenheimer approximation (BOMD). Following previous work [3], we fixed the substrate C atoms and performed the MD simulation under T = 6,000 K to mimic the impact of electron beam illumination. For diffusion barrier calculations, the nudged elastic band (NEB) approach [22] with eight images is employed to search the optimal diffusion.

Author contributions

The experiments were conceived by M. H. R. and A. B.. The TEM experiments were conducted by M. H. R. and A. B.. The TEM data preparation and image simulations were conducted by H. Q. T. and L. Z.. Theoretical calculations where conducted by W. Y.. All authors contributed to the data analysis and manuscript preparation.

Acknowledgements

The following are gratefully acknowledged. The National Natural Science Foundation of China (No. 51672181), the National Science Center for the financial support within the frame of the Sonata Program (No. 2014/13/D/ST5/02853) and the Opus program (No. 2015/19/B/ST5/03399). H. Q. T. thanks Soochow University for support. P. O. Å. P. wishes to acknowledge the Knut and Alice Wallenberg foundation for support of the electron microscopy laboratory in Linköping.

Electronic Supplementary Material: Supplementary material (more TEM images) is available in the online version of this article at https://doi.org/10.1007/s12274-017-1861-3.

References

[1] Rümmeli, M. H.; Rocha, C. G.; Ortmann, F.; Ibrahim, I.; Sevincli, H.; Börrnert, F.; Kunstmann, J.; Bachmatiuk, A.; Pötsche, M.; Shiraishi, M. et al. Graphene: Piecing it together. *Adv. Mater.***2011**, *23*, 4471–4490.

[2] Al-Dulaimi, N.; Lewis, E. A.; Lewis, D. J.; Howell, S. K.; Haigh, S. J.; O'Brien, P. Sequential bottom-up and top-down processing for the synthesis of transition metal dichalcogenide nanosheets: The case of rhenium disulfide (ReS_2). *Chem. Commun*. **2016**, *52*, 7878–7881.

[3] Zhao, J.; Deng, Q.; Avdoshenko, S. M.; Fu, L.; Eckert, J.; Rümmeli, M. H. Direct *in situ* observations of single Fe atom catalytic processes and anomalous diffusion at graphene edges. *Proc. Natl. Acad. Sci. USA* **2014**, *111*, 15641–15646.

[4] Qiao, B.; Wang, A. Q.; Yang, X. F.; Allard, L. F.; Jiang, Z.; Cui, Y. T.; Liu, J. Y.; Li, J.; Zhang T. Single-atom catalysis of CO oxidation using Pt_1/FeO_x. *Nat. Chem.***2011**, *3*, 634–641.

[5] Sun, S. H.; Zhang, G. X.; Gauquelin, N.; Chen, N.; Zhou, J. G.; Yang, S. L.; Chen, W. F.; Meng, X. B.; Geng, D. S.; Banis, M. N. et al. Single-atom catalysis using Pt/graphene achieved through atomic layer deposition. *Sci. Rep.* **2013**, *3*, 1775–1784.

[6] Sun, L. T.; Banhart, F.; Warner, J. Two-dimensional materials under electron irradiation. *MRS Bull.* **2015**, *40*, 29–37.

[7] Ramasse, Q. M.; Zan, R.; Bangert, U.; Boukhvalov, D. W.; Son, Y. W.; Novoselov, K. S. Direct experimental evidence of metal-mediated etching of suspended graphene. *ACS Nano* **2012**, *6*, 4063–4071.

[8] Wang, W. L.; Santos, E. J. G.; Jiang, B.;Cubuk, E. D.; Ophus, C.; Centeno, A.; Pesquera, A.; Zurutuza, A.; Ciston, J.; Westervelt, R. et al. Direct observation of a long-lived single-atom catalyst chiseling atomic structures in graphene. *Nano Lett.* **2014**, *14*, 450–455.

[9] Robertson, A. W.; Montanari, B.; He, K.; Kim, J.; Allen, C. S. Wu, Y. A.; Olivier, J.; Neethling, J.; Harrison, N.; Kirkland, A. I. et al. Dynamics of single Fe atoms in graphene vacancies. *Nano Lett.* **2013**, *13*, 1468–1475.

[10] Zhao, L.; Ta, H. Q.; Dianat, A.; Soni, A.; Fediai, A.; Yin, W. J.; Gemming, T.; Trzebicka, B.; Cuniberti, G.; Liu, Z. F. et al. *In situ* electron driven carbon nanopillar-fullerene transformation through Cr atom mediation. *Nano Lett.* **2017**, *17*, 4725–4732.

[11] Liu, Y. Y.; Dobrinsky, A.; Yakobson, B. I. Graphene edge from armchair to zigzag: The origins of nanotube chirality? *Phys. Rev. Lett.* **2010**, *105*, 235502.

[12] Warner, J. H.; Rümmeli, M. H.; Ge, L.; Gemming, T.; Montanari, B.; Harrison, N. M.; Büchner, B.; Briggs, G. A. D. Structural transformations in graphene studied with high spatial and temporal resolution. *Nat. Nanotechnol.* **2009**, *4*, 500–504.

[13] Hernadia, K.; Fonseca, A.; Nagya, J. B.; Bernaerts, D.; Lucas, A. A. Fe-catalyzed carbon nanotube formation. *Carbon* **1996**, *34*, 1249–1257.

[14] Rümmeli, M. H.; Schäffel, F.; Kramberger, C.; Gemming, T.; Bachmatiuk, A.; Kalenczuk, R. J.; Rellinghaus, B.; Büchner, B.; Pichler, T. Oxide-driven carbon nanotube growth in supported catalyst CVD. *J. Am. Chem. Soc.* **2007**, *129*, 15772–15773.

[15] An, H.; Lee, W. J.; Jung, J. Graphene synthesis on Fe foil using thermal CVD. *Curr. Appl. Phys.* **2011**, *11*, S81–S85.

[16] Baker, R. T. K.; Harris, P. S.; Thomas, R. B.; Waite, R. J. Formation of filamentous carbon from iron, cobalt and chromium catalyzed decomposition of acetylene. *J. Catal.* **1973**, *30*, 86–95.

[17] Robertson, J.; Hofmann, S.; Cantoro, M.; Parvez, A.; Ducati, C.; Zhong, G.; Sharma, R.; Mattevi, C. Controlling the catalyst during carbon nanotube growth. *J. Nanosci. Nanotechnol.* **2008**, *8*, 6105–6111.

[18] Ta, H. Q.; Perello, D. J.; Duong D. L.; Han G. H.; Gorantla S.; Nguyen V. L.; Bachmatiuk, A.; Rotkin, S.V.; Lee, Y. H.; Rümmeli, M. H. Stranski−krastanov and volmer−weber CVD growth regimes to control the stacking order in bilayer graphene. *Nano Lett.* **2016**, *16*, 6403–6410.

[19] Kresse, G.; Furthmüller, J. Efficient iterative schemes for *ab initio* total-energy calculations using a plane-wave basis set. *Phys. Rev. B* **1996**, *54*, 11169–11186.

[20] Kresse, G.; Furthmüller, J. Efficiency of *ab-initio* total energy calculations for metals and semiconductors using a plane-wave basis set. *Comput. Mater. Sci.* **1996**, *6*, 15–50.

[21] Perdew, J. P.; Burke, K.; Ernzerhof, M. Generalized gradient approximation made simple. *Phys. Rev. Lett.* **1996**, *77*, 3865–3868.

[22] Mills, G.; Jónsson, H.; Schenterb, G. K. Reversible work transition state theory: Application to dissociative adsorption of hydrogen. *Surf. Sci.* **1995**, *324*, 305–337.